

Exoplanets Characterization

Planets and Astrobiology (2020-2021)

G. Vladilo

Exoplanets characterization

- Study of the physical properties of individual planets
 - Direct imaging can provide experimental data useful to characterize individual planets
 - In general, the best way to constrain the properties of individual exoplanets is to combine different observational techniques
 - From this combination of experimental data, with the aid of modelization, we can derive information on
 - Planetary interiors
 - Planetary atmospheres
 - Planetary energy budget

Combination of different observational methods

- Doppler + transit methods

- Combines the mass obtained from the Doppler method with the radius obtained with the transit method
- The degeneration of the orbital inclination $\sin i$ is solved

Can provide a large number of exoplanets, as long as the targets are sufficiently bright for high-resolution spectroscopy

- Doppler + astrometric methods

- Given the minimum mass $M \sin i$ from the Doppler method, one can in principle estimate $\sin i$ with the astrometric method; in this way one can obtain the mass, rather than the minimum mass

Currently limited due to the difficulty of astrometric observations

Estimate of planetary masses from Transit Timing Variations

Technique that can be applied to multiple planetary systems discovered with the transit method

In a planetary system with many planets in nearby orbits, gravitational perturbations will induce small variations in the timing of the transits

– From a detailed analysis of the transit timings it is possible to deduce the mass of the planets, even without radial velocity observations

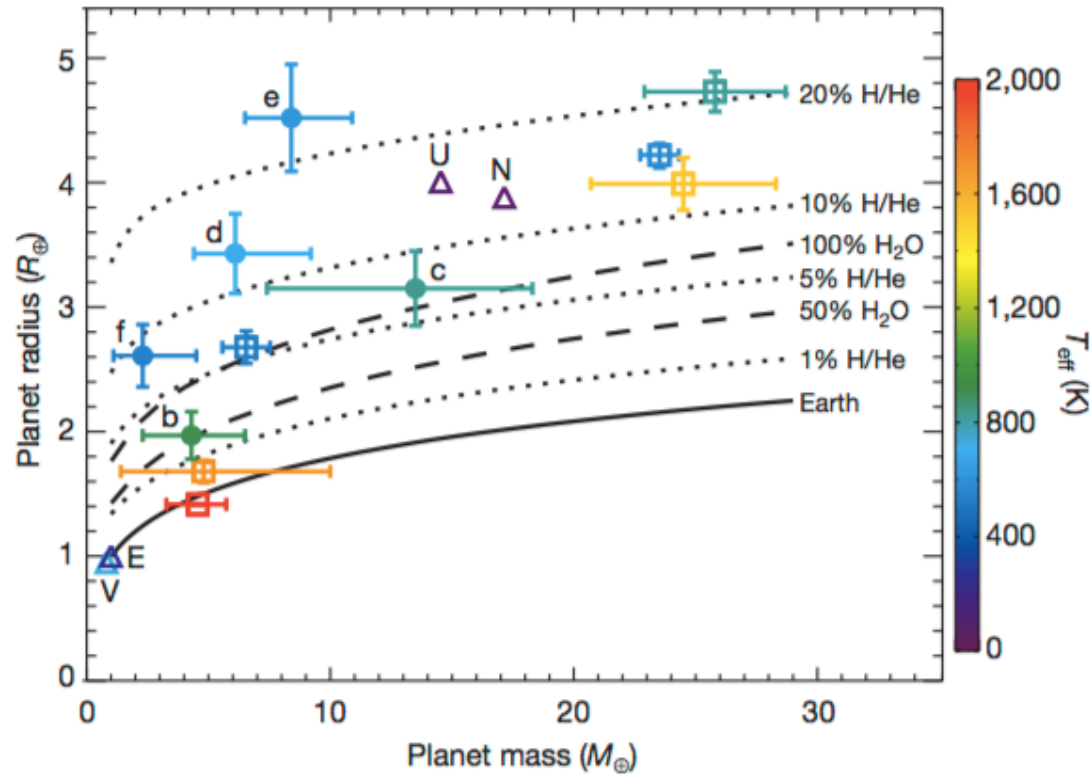
Examples:

– Kepler-11 (Lissauer et al. 2011)

– Trappist 1 (Gillon et al. 2017)

Kepler-11 (Lissauer et al. 2011)

Planet	Period (days)	Epoch (BJD)	Semi-major axis (AU)	Inclination (°)	Transit duration (h)	Transit depth (millimagnitude)	Radius (R_{\oplus})	Mass (M_{\oplus})	Density (g cm^{-3})
b	10.30375 ± 0.00016	$2,454,971.5052 \pm 0.0077$	0.091 ± 0.003	$88.5^{+1.0}_{-0.6}$	4.02 ± 0.08	0.31 ± 0.01	1.97 ± 0.19	$4.3^{+2.2}_{-2.0}$	$3.1^{+2.1}_{-1.5}$
c	13.02502 ± 0.00008	$2,454,971.1748 \pm 0.0031$	0.106 ± 0.004	$89.0^{+1.0}_{-0.6}$	4.62 ± 0.04	0.82 ± 0.01	3.15 ± 0.30	$13.5^{+4.8}_{-6.1}$	$2.3^{+1.3}_{-1.1}$
d	22.68719 ± 0.00021	$2,454,981.4550 \pm 0.0044$	0.159 ± 0.005	$89.3^{+0.6}_{-0.4}$	5.58 ± 0.06	0.80 ± 0.02	3.43 ± 0.32	$6.1^{+3.1}_{-1.7}$	$0.9^{+0.5}_{-0.3}$
e	31.99590 ± 0.00028	$2,454,987.1590 \pm 0.0037$	0.194 ± 0.007	$88.8^{+0.2}_{-0.2}$	4.33 ± 0.07	1.40 ± 0.02	4.52 ± 0.43	$8.4^{+2.5}_{-1.9}$	$0.5^{+0.2}_{-0.2}$
f	46.68876 ± 0.00074	$2,454,964.6487 \pm 0.0059$	0.250 ± 0.009	$89.4^{+0.3}_{-0.2}$	6.54 ± 0.14	0.55 ± 0.02	2.61 ± 0.25	$2.3^{+2.2}_{-1.2}$	$0.7^{+0.7}_{-0.4}$
g	118.37774 ± 0.00112	$2,455,120.2901 \pm 0.0022$	0.462 ± 0.016	$89.8^{+0.2}_{-0.2}$	9.60 ± 0.13	1.15 ± 0.03	3.66 ± 0.35	<300	–



Planets with measurements of masses and radii

From mass and radius measurement we obtain

– mean density $\rho \sim M/R^3$

With the aid of models of planetary interiors, ρ casts light on the internal structure/composition of the planet

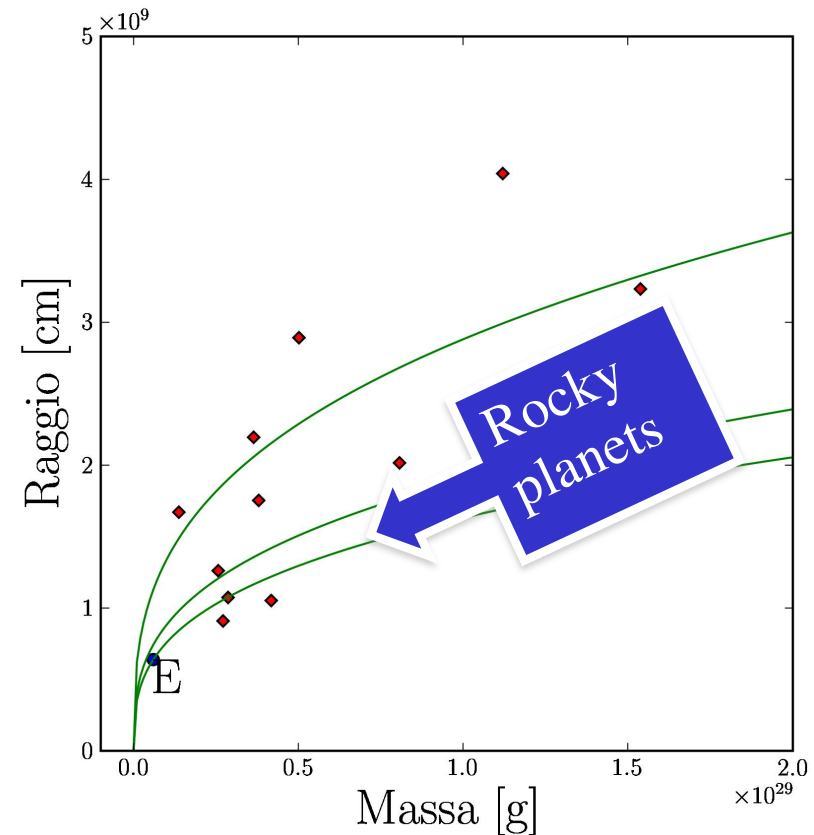
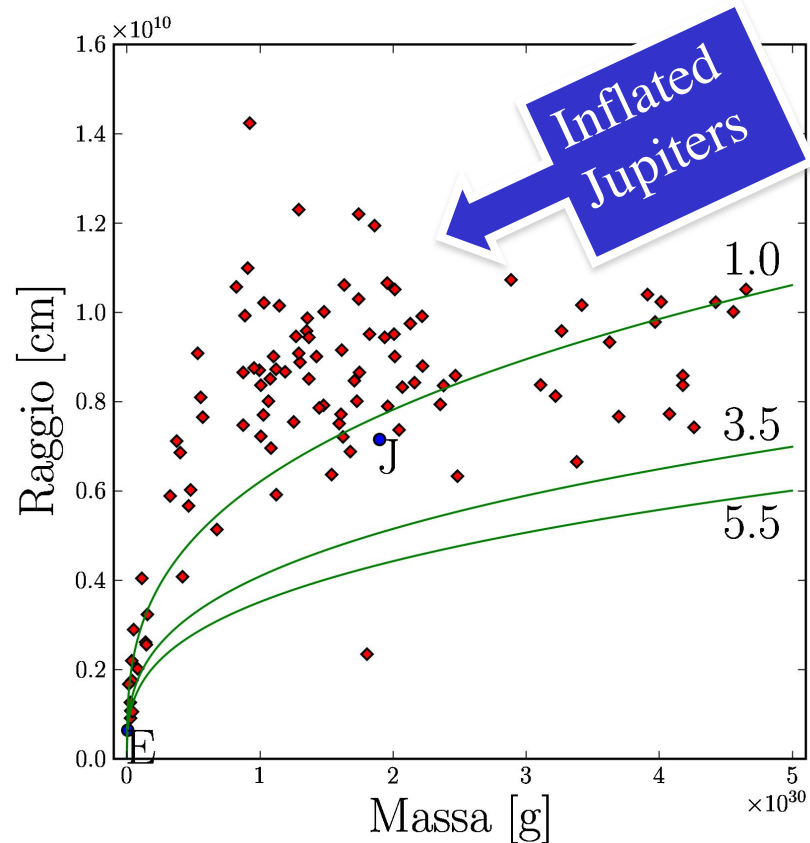
– surface gravity $g \sim M/R^2$

Important for the modelization of the atmosphere and climate

– escape velocity $v_e \sim (M/R)^{1/2}$

Indicates the capacity for the planet to maintain an atmosphere

By comparing masses and radii with curves of equal mean density one can cast light on the bulk composition



Green curves: lines of uncorrected constant mean density
Most exoplanets discovered so far are gaseous ($\rho < 1 \text{ g cm}^{-3}$),
but we are starting to discover rocky ones ($\rho > 3 \text{ g cm}^{-3}$)

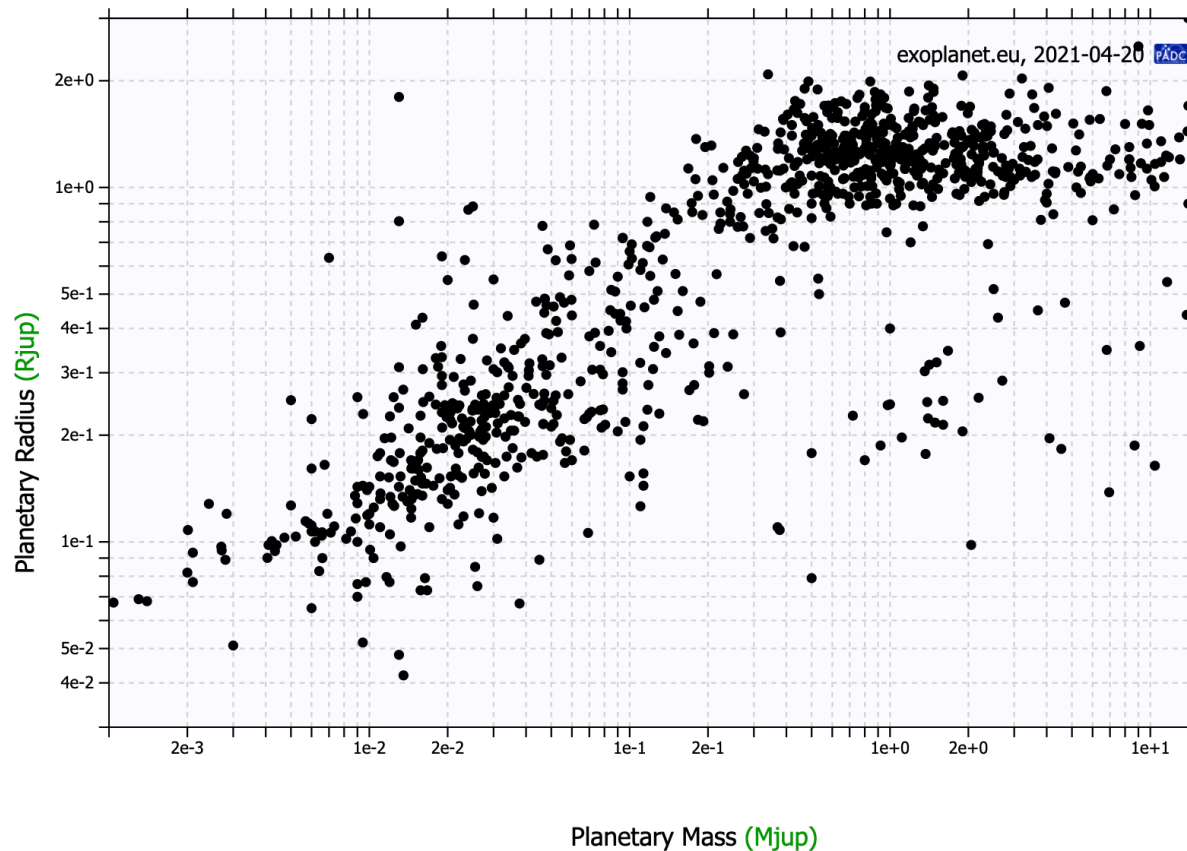
Mass versus radius: experimental data

For low-mass planets, the radius increases faster than $R \sim (M/\rho)^{1/3}$
i.e., faster than expected for the case of constant mean density

Interpretation:

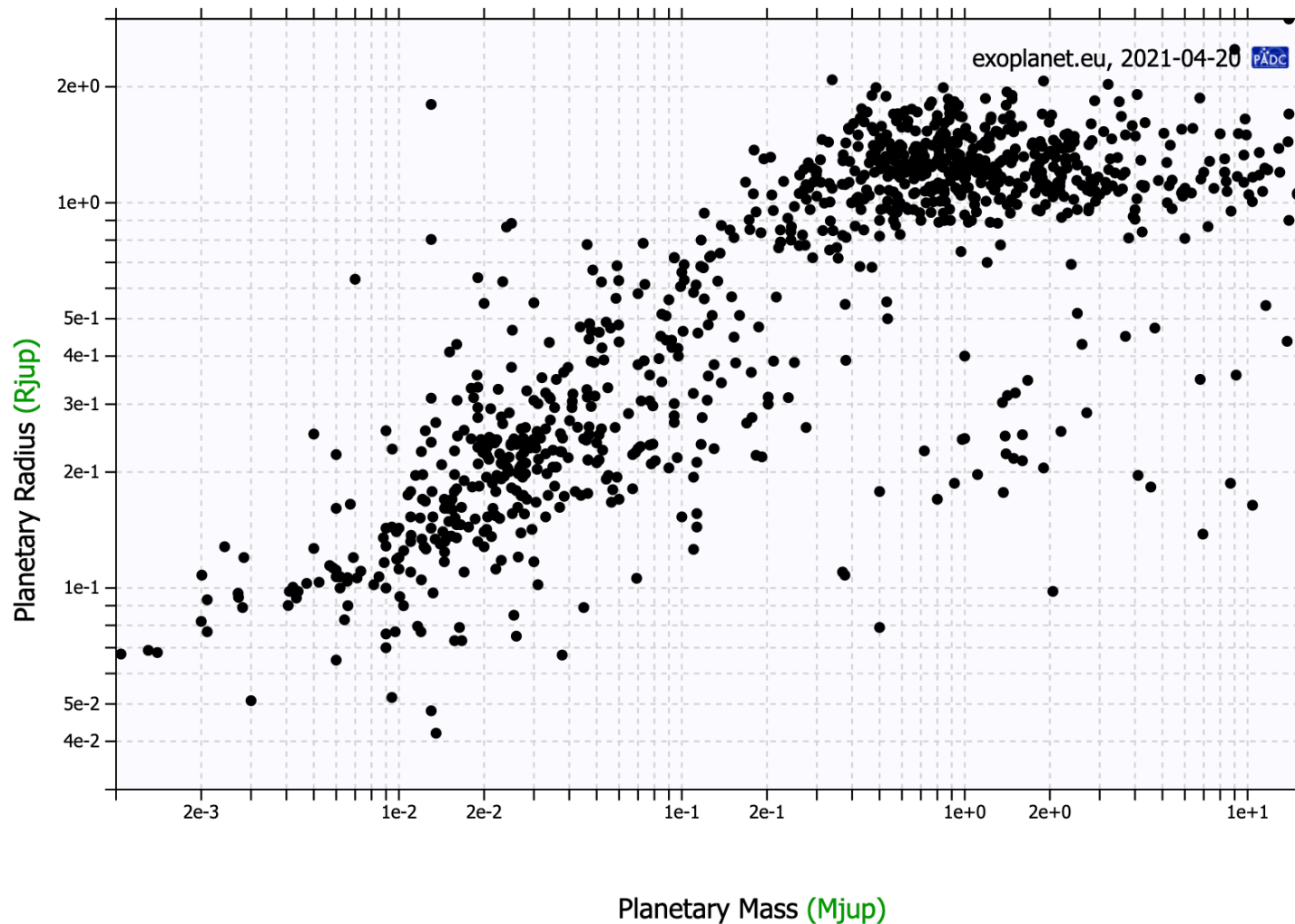
In the early stages of planetary formation the planets accrete dense (refractory) material, whereas at later stages low-density (volatile) material

As a result, the mean density decreases as the accumulated mass (or size) increases



Mass versus radius: experimental data

For high-mass planets, the radius does not increase significantly with mass
Above some critical point, the process of planetary formation becomes different

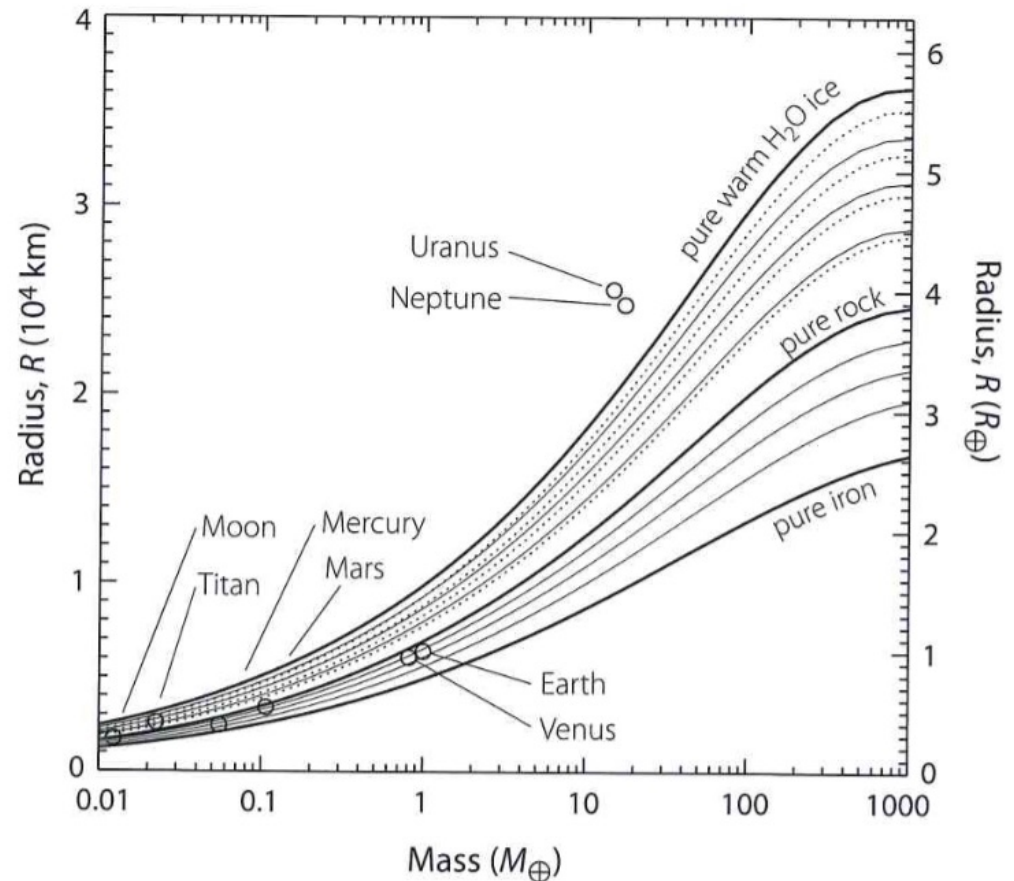


Mass versus radius: theoretical relations for planets of low mass

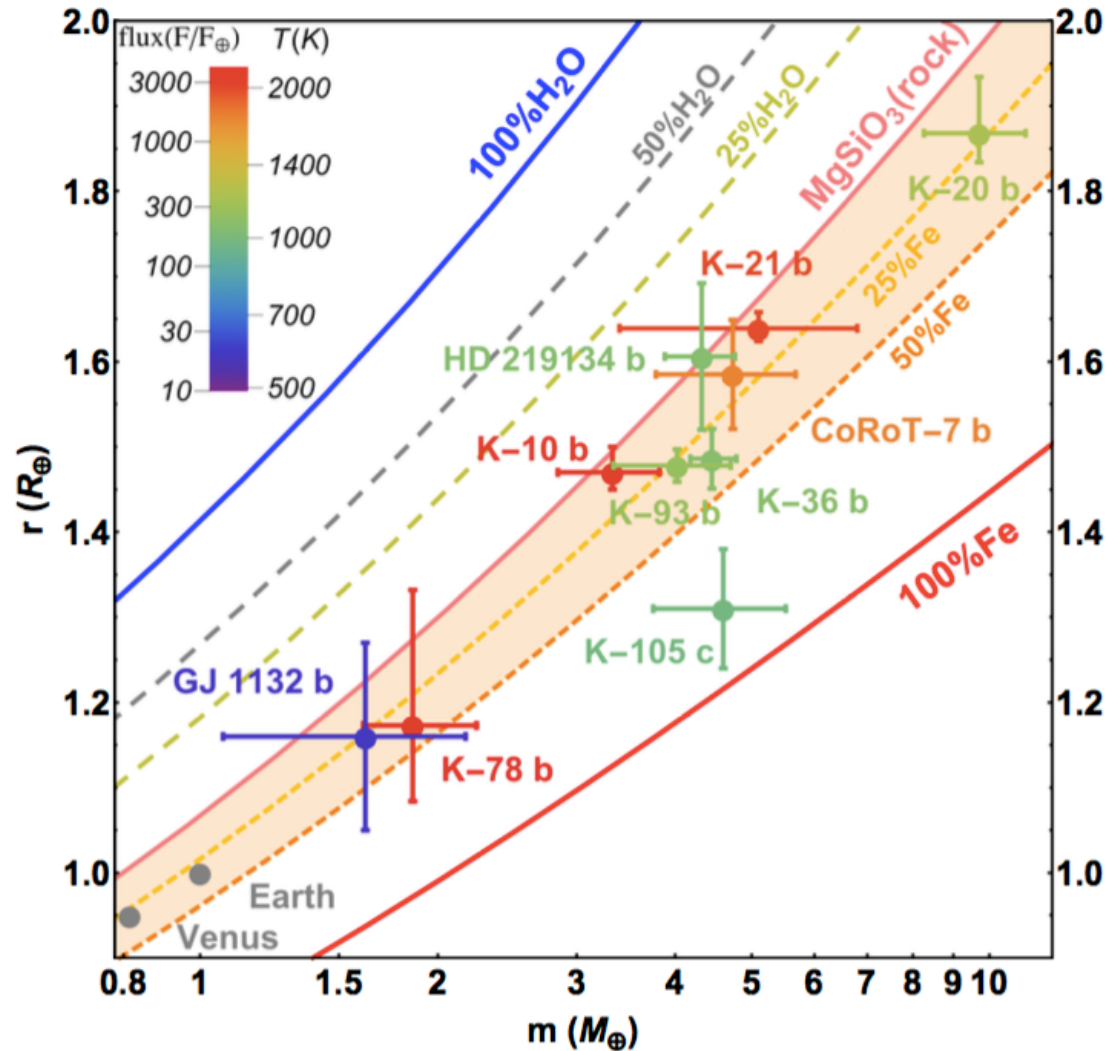
Mass versus radius for planets composed of H₂O ice, rock (Mg₂SiO₄), and iron

Thin curves are calculated for different values of fractional composition and different temperatures

From Fortney et al. 2007)



Zeng et al. (2017)



Mass-radius plots showing selected rocky planets

Curves show models with different compositions

Planets are color-coded according to their incident stellar flux

Mean density versus radius and insolation

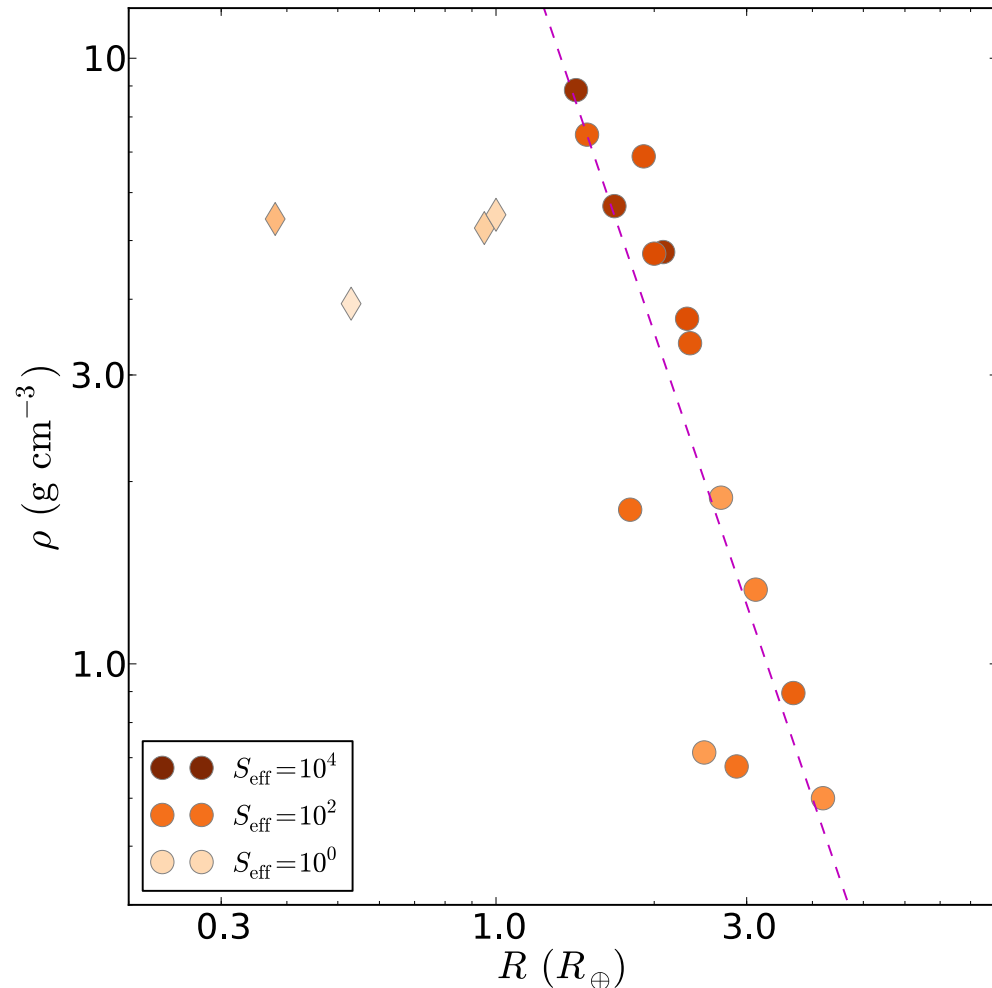
Sample of planets with
 $M < 10$ Earth masses
and reliable measurements of M and R

- The uncorrected mean density decreases with increasing planet size (dashed line)
- The level of insolation tends to decrease with decreasing density
 - This implies that the insolation plays an important role in the process of planetary accretion

Possible interpretation:

When the insolation is high only dense, refractory material is accumulated

Circles: exoplanets
Diamonds: Solar System planets
Color coding: insolation

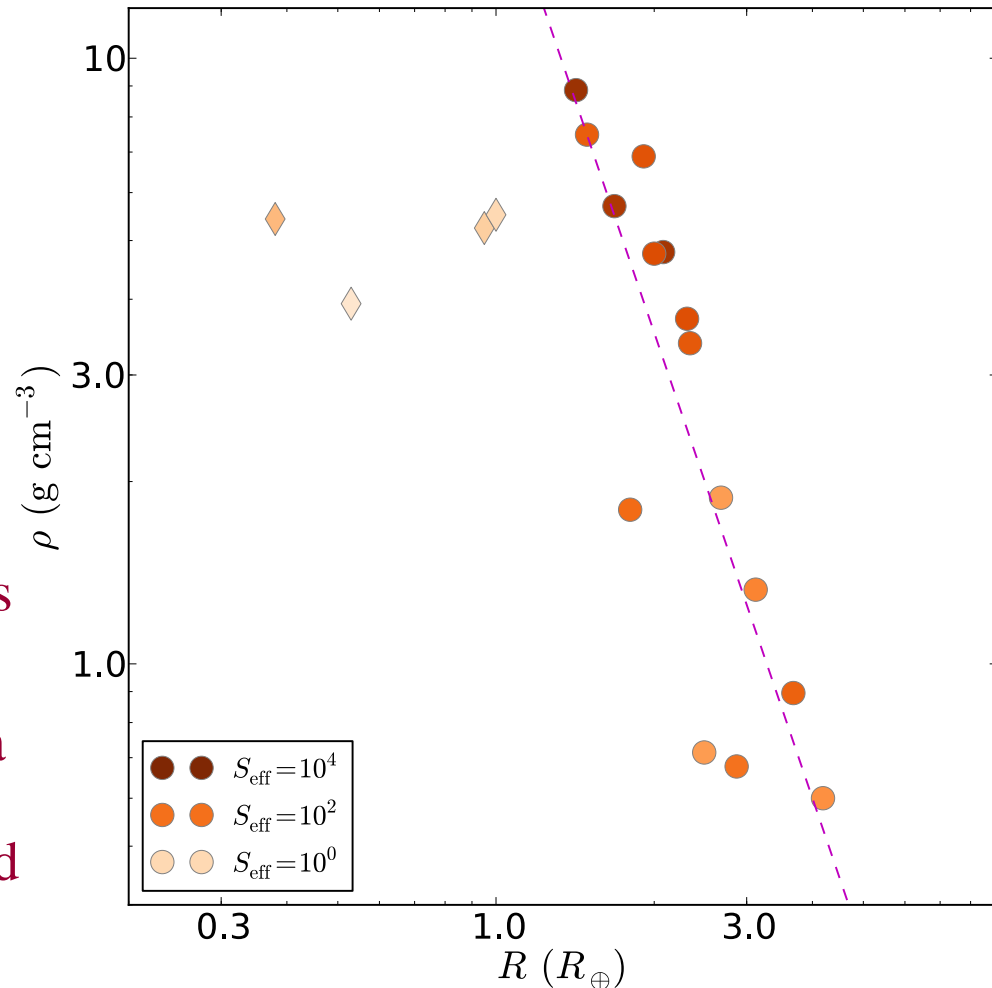


Mean density versus radius and insolation

Sample of planets with
 $M < 10$ Earth masses
and reliable measurements of M and R

- Solar System planets do not follow the experimental trend observed in exoplanets
- At a given density and radius, their level of insolation is much lower
- Current samples of exoplanets are not representative of Solar System conditions, even when we consider planets with similar radii and densities
- This situation will change when data of terrestrial-type planets with lower level of insolation will be accumulated

Circles: exoplanets
Diamonds: Solar System planets
Color coding: insolation



The trends are different at low and high values of planetary radius
 The change of slope takes place at $R \sim 1.6 R_{\text{earth}}$

Weiss & Marcy (2014)

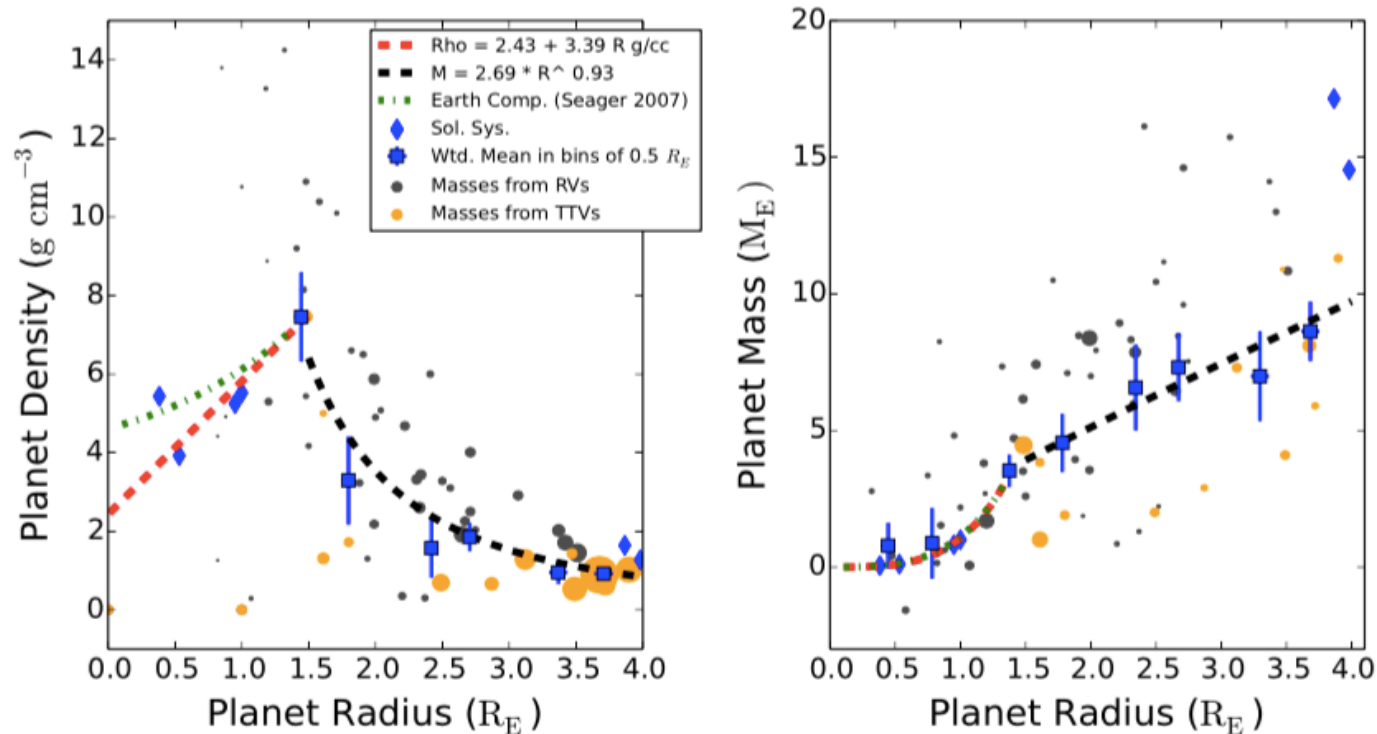


Figure 2. Left: density vs. radius for 65 exoplanets. Gray points have RV-determined masses, orange points have TTV-determined masses, and the point size corresponds to $1/\sigma(\rho_p)$. The blue squares are weighted mean densities in bins of $0.5 R_{\oplus}$, with error bars representing $\sigma_i/\sqrt{N_i}$, where σ_i is the standard deviation of the densities and N_i is the number of exoplanets in bin i . We omit the weighted mean densities below $1.0 R_{\oplus}$ because the scatter in planet densities is so large that the error bars span the range of physical densities ($0\text{--}10 \text{ g cm}^{-3}$). The blue diamonds indicate solar system planets. The red line is an empirical density–radius fit for planets smaller than $1.5 R_{\oplus}$, including the terrestrial solar system planets. The green line is the mass–radius relation from Seager et al. (2007) for planets of Earth composition (67.5% MgSiO_3 , 32.5% Fe). The increase in planet density with radius for $R_p < 1.5 R_{\oplus}$ is consistent with a population of rocky planets. Above $1.5 R_{\oplus}$, planet density decreases with planet radius, indicating that as planet radius increases, so does the fraction of gas. Right: mass vs. radius for 65 exoplanets. Same as left, but the point size corresponds to $1/\sigma(M_p)$ and the blue squares are the weighted mean masses in bins of $0.5 R_{\oplus}$, with error bars representing $\sigma_i/\sqrt{N_i}$, where σ_i is the standard deviation of the masses and N_i is the number of exoplanets in bin i . The black line is an empirical fit to the masses and radii above $1.5 R_{\oplus}$; see Equation (3). The weighted mean masses were not used in calculating the fit. Some mass and density outliers are excluded from these plots, but are included in the fits.

Ocean planets

The large variety of exoplanet properties suggests that planets with masses in the range between Earths and super-Earths may have bulk composition dominated by volatiles, such as H₂O ice, rather than rocky material

Such objects, called ocean planets, could form at large orbital distances, beyond the snow line

In the range 1- 10 Earth masses they are not expected to accumulate a large H/He envelope (at variance with icy/gaseous giants of the Solar System)

A fraction of such planets could have migrated inwards, in a region where water can be in liquid phase, leading to the existence of “water worlds”

Candidate ocean planet:

example: GJ 1214 b ($d=13$ pc, $M=6.6M_{\oplus}$, $R=2.7R_{\oplus}$, $\rho=1.9$ g cm⁻³)

Exoplanet characterization:

Observations of the radiation emitted by the planet

- The faint radiation emitted by planets has two contributions
 - Intrinsic thermal emission
 - The thermal emission can be observed in the *infrared* band
 - Provides information on the planet surface temperature and the atmospheric properties of the outer layers
 - Reflected stellar radiation
 - The stellar light reflected by the planet can be observed in the *visible* band
 - Provides information on the albedo properties of the outer layers

Exoplanet characterization:

Observations of the radiation emitted by the planet

- Methods to measure the exoplanet radiation

- Direct imaging

If the image of the planet is solved, the thermal emission can be directly measured

In this case, however, the planet-star separation will be quite high and, as a result, the stellar light reflected by the planet cannot be measured

- Secondary transits

By studying the light curve at the epoch in which the planet is hidden by the star (“secondary transit”)

Effective temperatures derived from the thermal emission of exoplanets by means of direct imaging

Masses can be estimated from models of planetary evolution

Exoplanet Roadmap Advisory Team (ESA)

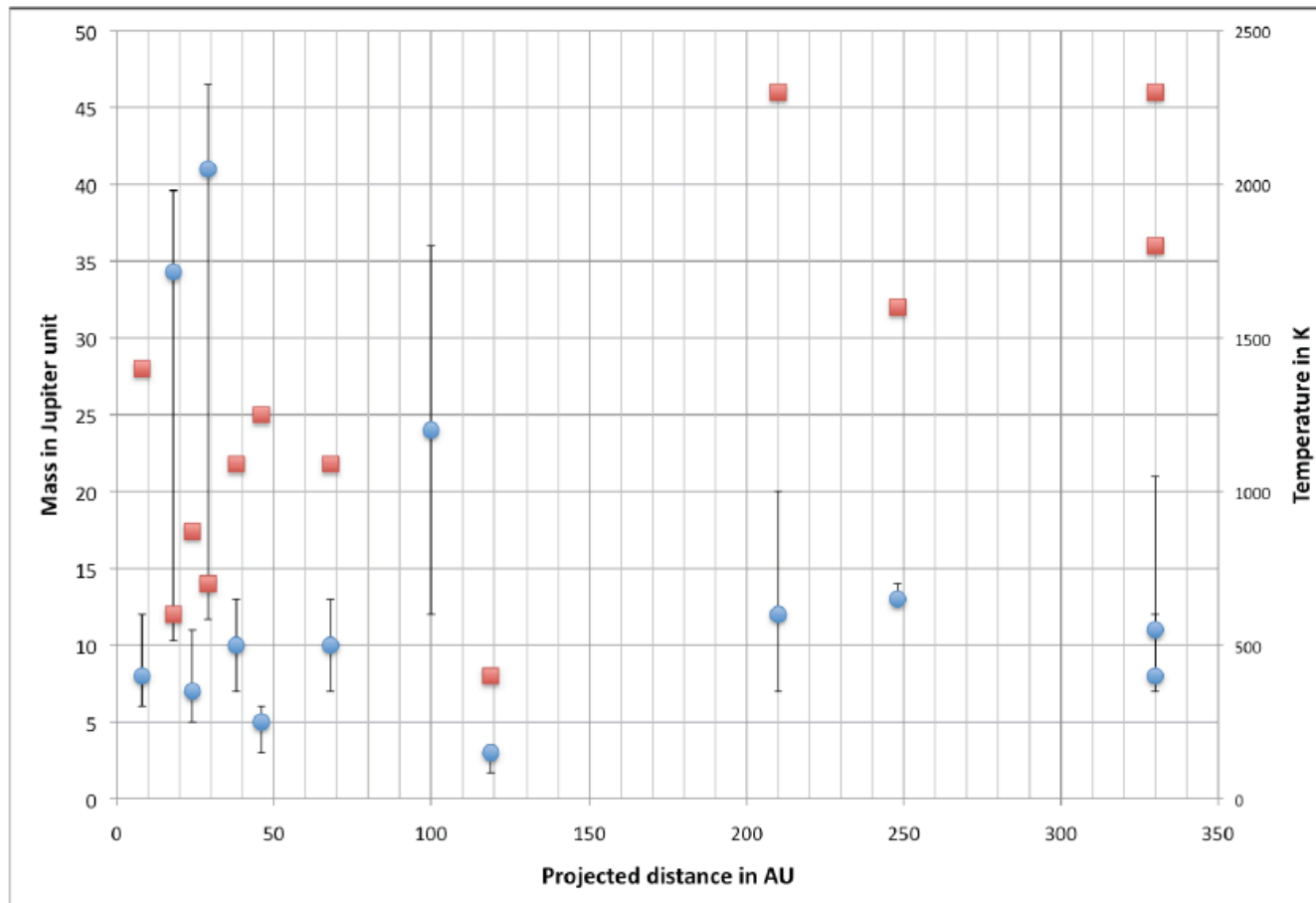
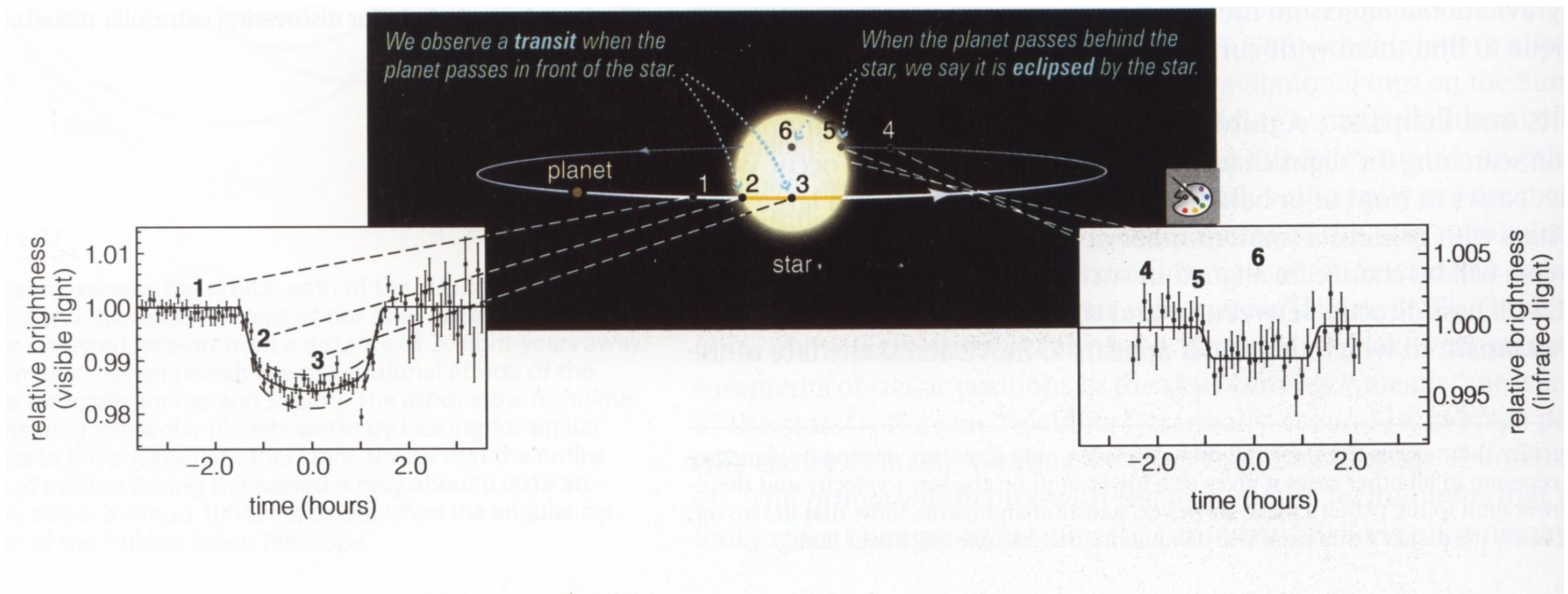


Fig. 2 : Estimated mass (blue dots) and temperature (red squares) vs. separation diagram of young planet candidates found by direct imaging.

Secondary transits

Secondary transit (or eclipse)

- Transit of the planet behind the star (the planet is eclipsed by the star)
- With a proper geometric configuration of the orbits



Secondary transits

Light curve of the secondary transit

- Out of the eclipse: sum of the stellar+planetary emission
 - During the eclipse: only the stellar emission
- As a result there is a small dip in the light curve

Importance of the secondary transit

- The difference of the fluxes during and out of the transit provides a direct measurement of the planetary emission
- The effect is stronger in the infrared and allows us to study the infrared emission of the planet

Secondary transits

In the Rayleigh-Jeans limit of the Plackian emission, valid at long wavelengths, the emission scales linearly with T , and the depth of the secondary eclipse is given by

$$\Delta F \simeq \frac{T_p}{T_\star} \left(\frac{R_p}{R_\star} \right)^2$$

The detection of secondary transits is biased in favour of hot, giant planets orbiting cool, dwarf stars

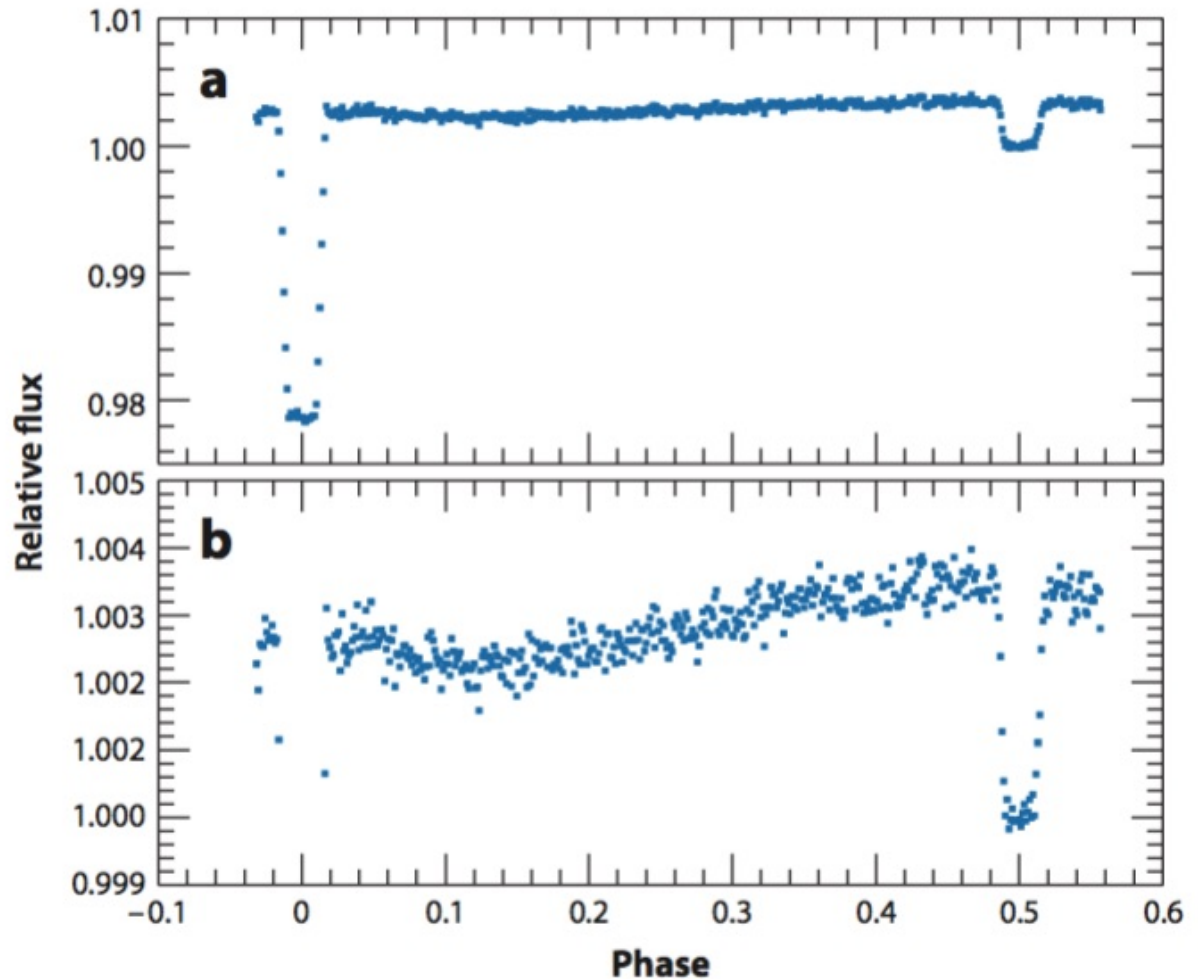
Secondary transits

Example:

Infrared light curve of
HD 189733A and b
(K1-K2 star at 19 pc,
 $M_p=1.15 M_J$, $a=0.03$ AU)

The first dip (left) is the
transit and the second dip
the secondary eclipse

Bottom panel: a zoom of
the top panel



Surface temperature distribution of tidally-locked Hot Jupiters

- For transiting Hot Jupiters the light curves of primary and secondary transits can be combined to derive information on the light emitted by the planet at different orbital phases
- Assuming that the planet is tidally locked, the orbital phase can be converted in phase of planetary rotation
- In this way it is possible to reconstruct the surface emissivity as a function of planet longitude

When the planet is exactly on the other side of the star, we observe the temperature of the sub-stellar point (the longitude that is constantly illuminated by the star)

At other orbital phases we measure the temperature of other longitudes

Surface temperature distribution of tidally-locked Hot Jupiters

Example:

- HD 189733b observed in the IR with Spitzer-IRAC (Knutson et al. 2007)
- The longitudinal variation of the surface temperature is not very high, in spite of the tidal locking
- The relatively small temperature variation suggests the existence of an efficient mechanism of heat diffusion along the planet surface
- There is an offset between the substellar point and the longitude of maximum temperature

